[Global Biogeochemical Cycles]

Supporting Information for

Decoupling of Barium and Silicon at the Congo River-dominated Southeast Atlantic Margin: Insights from Combined Barium and Silicon Isotopes

Zhouling Zhang[1*], Yang Yu[1], Ed C. Hathorne[1], Lucia H. Vieira[1], Patricia Grasse[1,2], Christopher Siebert[1], Peer Rahlf[1], Martin Frank[1]

[1]GEOMAR Helmholtz Centre for Ocean Research Kiel, Wischhofstr. 1-3, 24148 Kiel, Germany

[2]German Centre for Integrative Biodiversity Research (iDiv) Halle-Jena-Leipzig, Puschstrasse 4, 04103 Leipzig, Germany.

Corresponding author: Zhouling Zhang (zzhang@geomar.de)

Contents of this file

Additional Supporting Information (File uploaded separately)

Text S1. Hydrological setting of the Congo river estuary and Angola Basin

Due to the enrichment of particulate organic carbon (POC) in the suspended particles and dissolved organic carbon (DOC) in the dissolved load, the Congo River is the second largest exporter of terrestrial OC to the ocean after the Amazon (Cadée, 1978, 1984; Spencer et al., 2013). Discharge fluctuations in the Congo River are in general low both annually and interannually (Hughes et al., 2011; Spencer et al., 2013). The surface layer (~10 m) of river water travels within the central part of the plume maintained by a strong pycnocline and deepens to ~20 m in the mid-estuary. The plume starts as a jet stream of low-salinity, high-velocity waters invariably heading WNW nearshore. Beyond the mouth of the estuary, the plume (salinity <35) is diverted by seasonally shifting winds and is maintained as a low salinity surface lens heading west-north-west in November (Eisma & Van Bennekom, 1978). Congo plume waters are confined to the upper layer throughout the Southeastern Atlantic region and are decoupled from bottom influence due to the vertical stratification (Hopkins et al., 2013). The limitation of vertical mixing also restricts the supply of oxygen from the surface waters, leading to hypoxic and anoxic zones near the bottom (Vallaeys et al., 2021).

The Angola Basin is located in the Southeast Atlantic along the West African continental margin. The ocean currents at the continental margin represent a typical tropical eastern boundary circulation system dominated by the poleward-flowing Angola Current, which is fed by the eastward currents in the equatorial region (Mohrholz et al., 2001). Evaporation exceeds precipitation during the whole year in this region, leaving river runoff as the only explanation as a source for the freshwater anomaly in austral summer (Tchipalanga et al., 2018). The dominant continental freshwater source in this region is the Congo River, the discharge of which peaks from November to January (Dai et al., 2009). Major water masses in the northern Angola Basin are composed of Tropical Surface Water (TSW) at the uppermost 20 m, Subtropical Underwater (STUW) between about 20 and 100 m depth, South Atlantic Central Water (SACW) between about 100 and 500 m depth, Antarctic Intermediate Water (AAIW) below 500 m depth, Upper Circumpolar Deep Water (UCDW) below AAIW and North Atlantic Deep Water (NADW) in the deep and bottom waters (Rahlf et al., 2021). AABW is not present in our study area as the passage

of AABW into the Angola Basin is severely constrained by the barrier of the Walvis Ridge between the Cape and Angola basins (Chan et al., 1977).

Text S2. Details of Ba and Si isotopes analyses

The ^{130}Ba-^{135}Ba double spike was prepared from $^{130}BaCO_3$ and $^{135}BaCO_3$ (ORNL enriched to 35.8 and 93.4%, respectively). Water samples were spiked with a ^{130}Ba-^{135}Ba double spike in acid-cleaned Teflon and left on a hotplate at 80°C to equilibrate for at least 24 hours. Spike-equilibrated water samples were then transferred to acid-cleaned 10ml centrifuge tubes for co-precipitation after cooling down to room temperature. The pre-treated Ba-free Na_2CO_3 solution (1.1M, pH~12) was added to 10ml spiked seawater in 70ul increments up to 700ul with samples shaken vigorously between each Na_2CO_3 addition. The milky precipitate was left to settle overnight and collected at the base of the centrifuge tube after centrifuging at 4000 g for 10min. The precipitate was then directly dissolved in 1mL of 1M HCl and waited for loading. Ba was purified from the sample matrix using cation-exchange chromatography (BIORAD® AG50W-X8 resin, 200-400 μm mesh-size, 1.4 mL resin bed) twice with an average yield of 90% for the entire chemical preparation procedure. Briefly, matrix elements were subsequently eluted with 8 mL of 1 M HCl and 8 mL of 3 M HCl, respectively. The Ba cuts were then collected with 10 mL of 2 M HNO_3, dried, and re-dissolved in 2% (v/v) HNO_3 for Ba isotope analyses. The purified sample solutions were introduced as a dry aerosol into the plasma using an Aridus II desolvating system (CETAC Technologies, Omaha, NE, USA) equipped with an Aspire PFA micro-concentric nebulizer (uptake rate of ~50 μL min^{-1}). The MC-ICP-MS was tuned to a matrix tolerance state defined by a high Normalised Argon Index value (NAI, an index of plasma temperature) (Yu et al., 2020). The geometrical procedure described in (Siebert et al., 2001) was used for data reduction and each spiked sample measurement of δ^{138}Ba was normalized to two "bracketing" spiked standard measurements. The long-term reproducibility of repeated measurements of reference seawaters BATS 5m and BATS 2000m are shown in Fig. S1.

The analytical methods of dSi concentrations followed during the M121 GEOTRACES cruise correspond to those described by QuAAtro Applications. For Si isotopes measurement, during the brucite coprecipitation, the shaking time and settlement time were prolonged (2-5 hours shaking and 12-24 hours settling) to ensure the maximum co-precipitation for very low dSi concentration (<10) and very high dSi concentration (>100) samples. The least-squares linear regression between $\delta^{30}Si$ and $\delta^{29}Si$ is in excellent agreement and produces a slope of 0.518 (R^2 = 1.00; Fig. S1), which is indistinguishable from the theoretical values of equilibrium (0.518) and kinetic (0.505) fractionations (Young et al., 2002), indicating no polyatomic interferences during MC-ICP-MS measurements (Grasse et al., 2017).

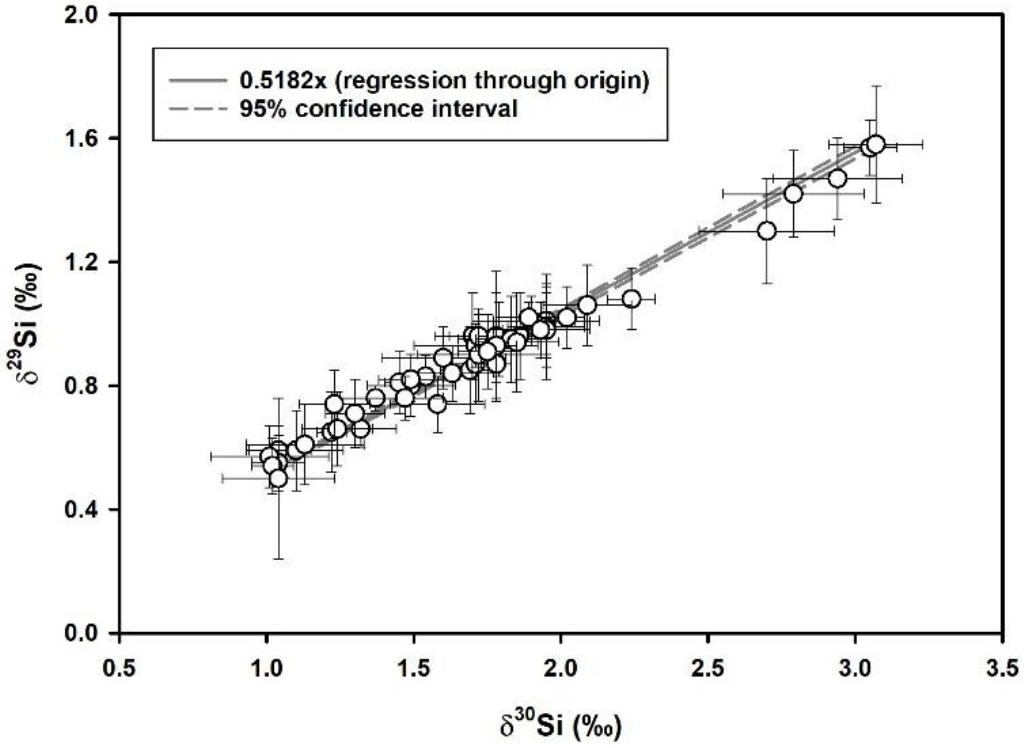

Figure S1: $\delta^{29}Si$ versus $\delta^{30}Si$ of all samples in this study.

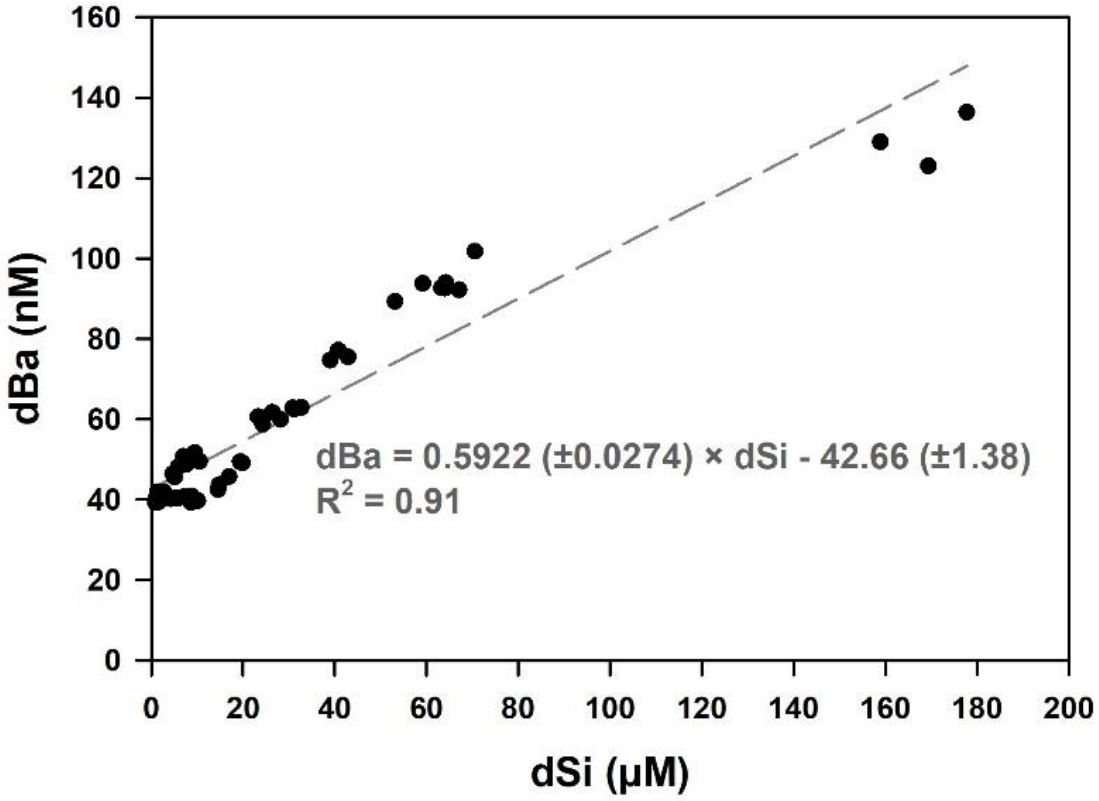

Figure S2. Element-element correlation plot of co-located dissolved Ba (dBa) and Si (dSi) in our study region

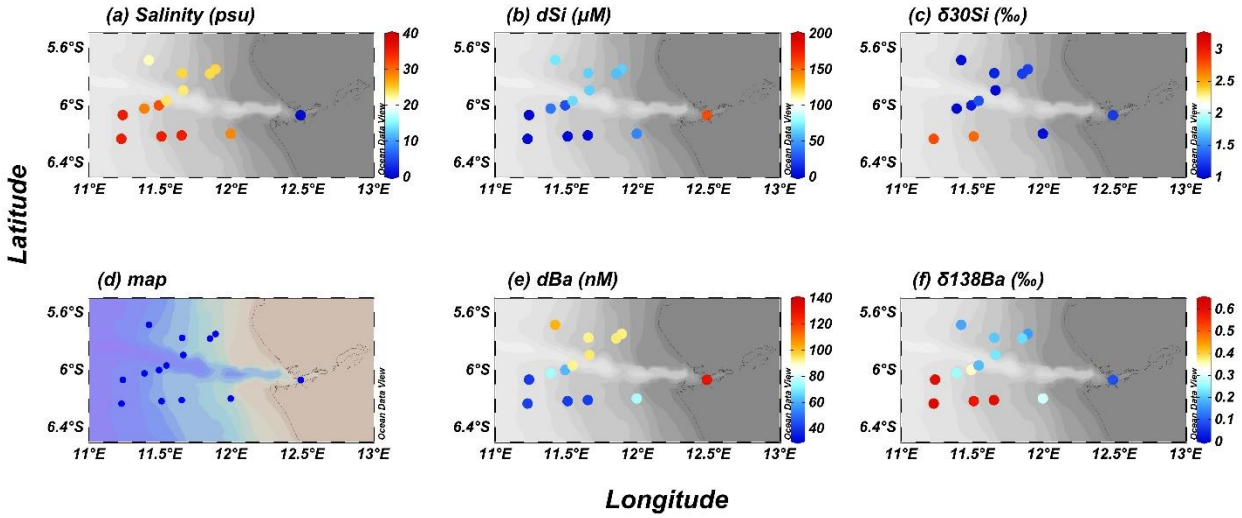

Figure S3. Surface distributions of (a) salinity, (b) dissolved silicate concentrations (dSi), (c) dissolved silicon isotopic compositions ($\delta^{30}Si$), (e) dissolved barium concentrations (dBa), and (f) dissolved barium isotopic compositions ($\delta^{138}Ba$) in the Congo River estuary. (d) shows the map of the sampling stations.

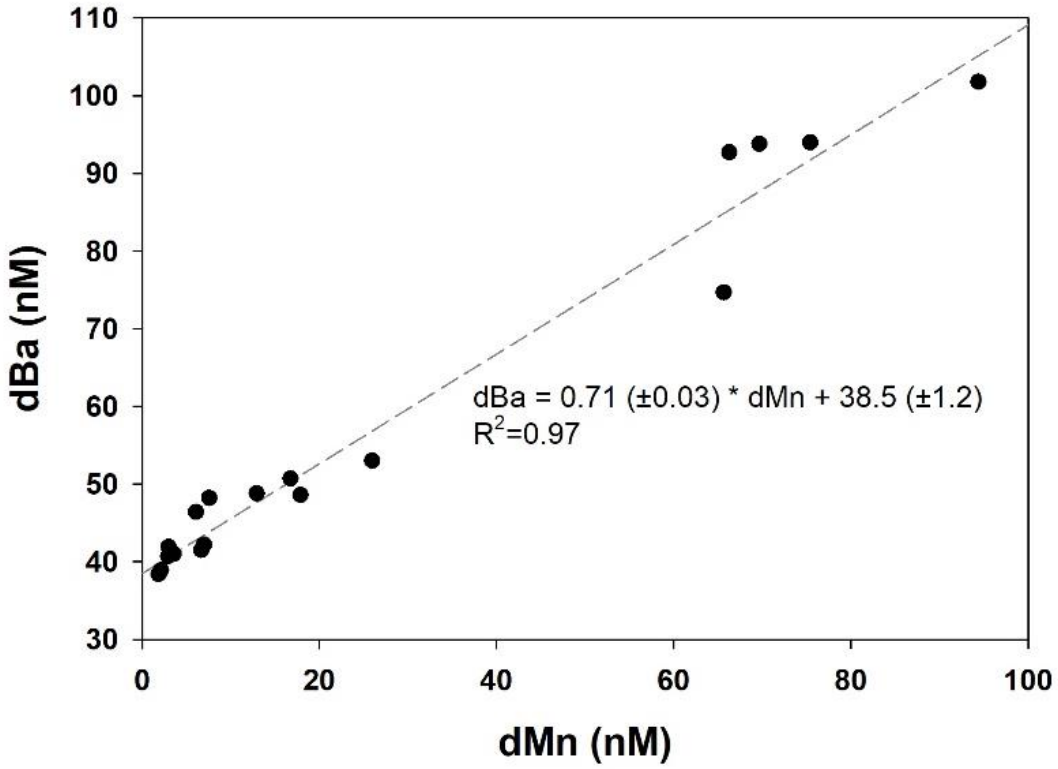

Figure S4. Element-element correlation plot of co-located dissolved Ba (dBa) and Mn (dMn) in the Congo plume. dMn data were previously published in Vieira et al., 2020.

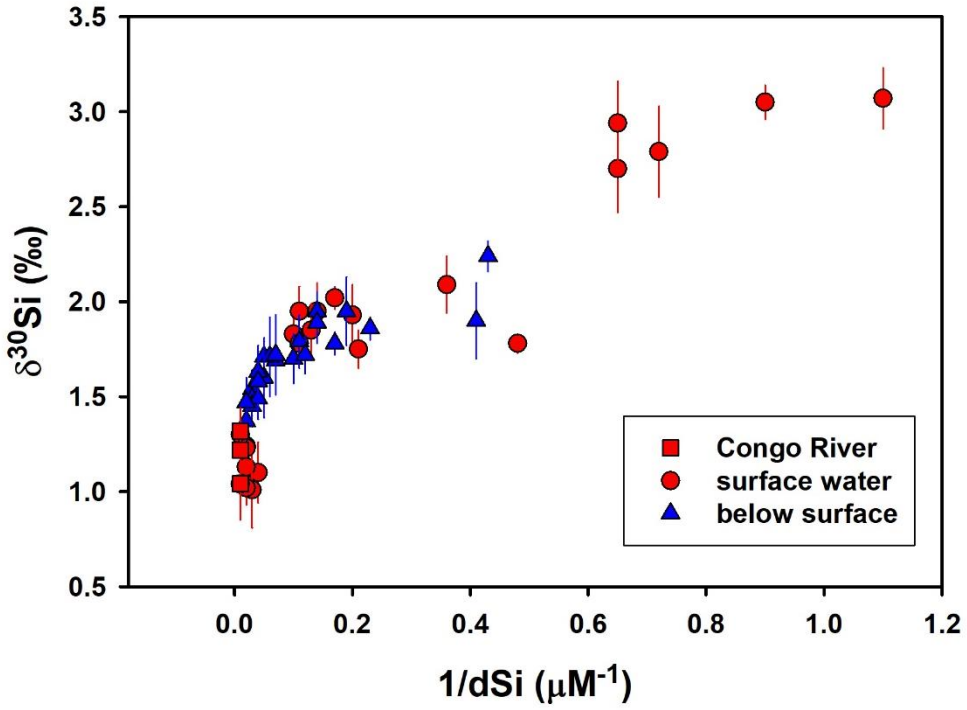

Figure S5. $\delta^{30}Si$ versus 1/dSi. Red squares, red circles, and blue triangles denote Congo River samples, surface FISH samples, and all the samples below the surface, respectively.

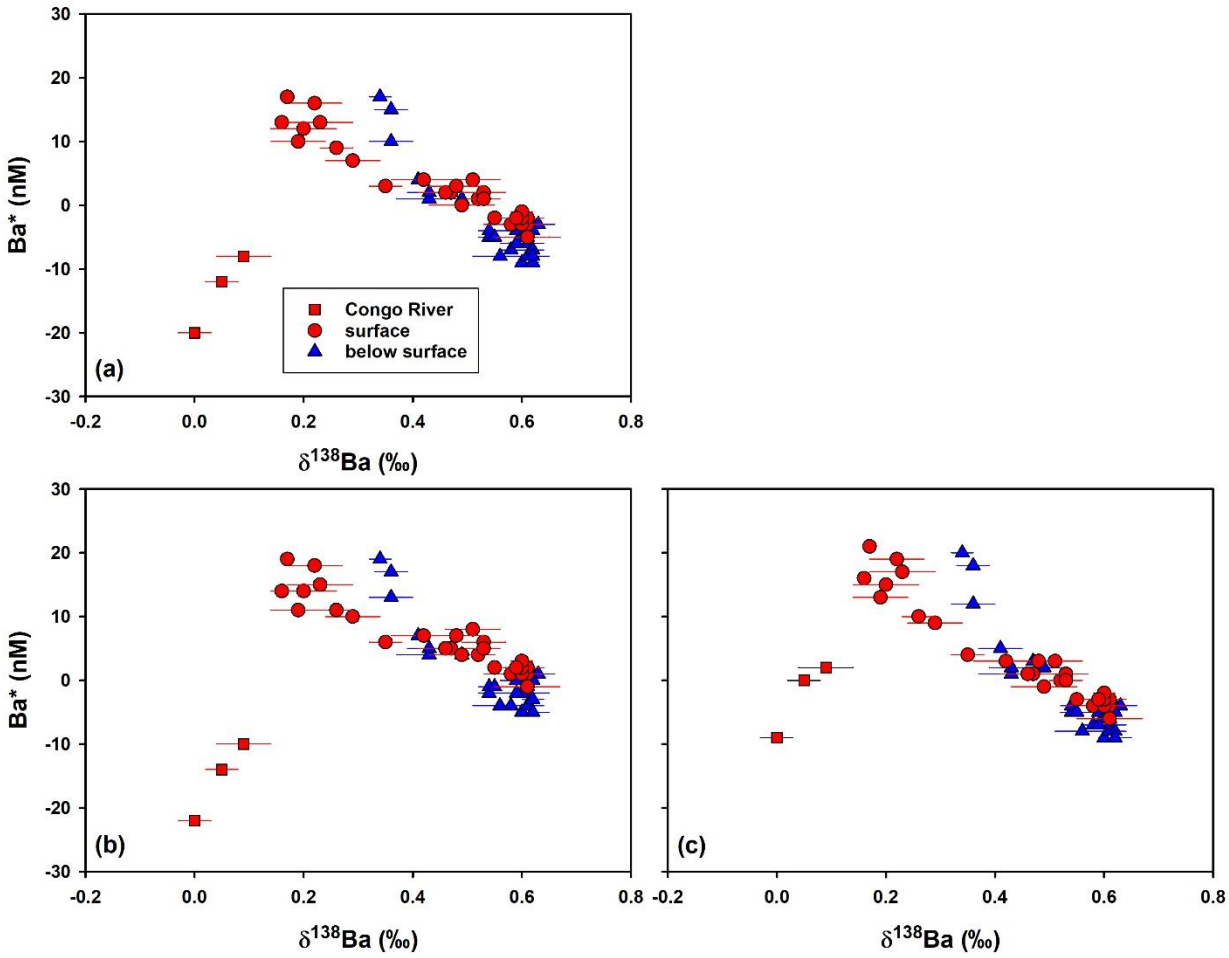

Figure S6. Comparison of Ba* versus δ^{138}Ba cross plots from all samples in this study calculated based on (a) the regional correlation: Ba* = dBa – 0.59 × dSi – 42.7, (b) the global correlation from Bates et al. (2017): Ba* = dBa – 0.63 × dSi – 38.6, and (c) the Atlantic correlation from Horner et al. (2015): Ba* = dBa – 0.52 × dSi – 43.9.

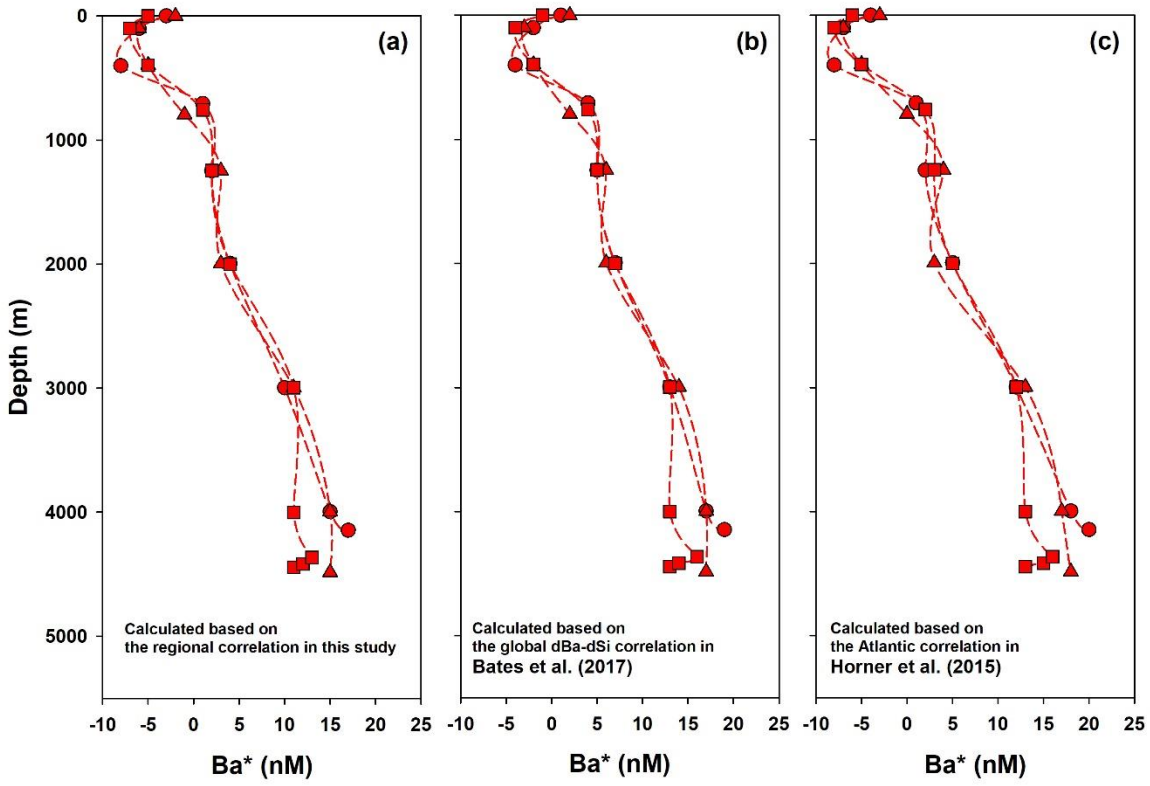

Figure S7. Comparison of Ba* at off-shelf stations (Stn.21: circle; Stn.22: triangle; Stn.24: square) based on (a) the regional correlation: Ba* = dBa – 0.59 × dSi – 42.7, (b) the global correlation from Bates et al. (2017): Ba* = dBa – 0.63 × dSi – 38.6, and (c) the Atlantic correlation from Horner et al. (2015): Ba* = dBa – 0.52 × dSi – 43.9.

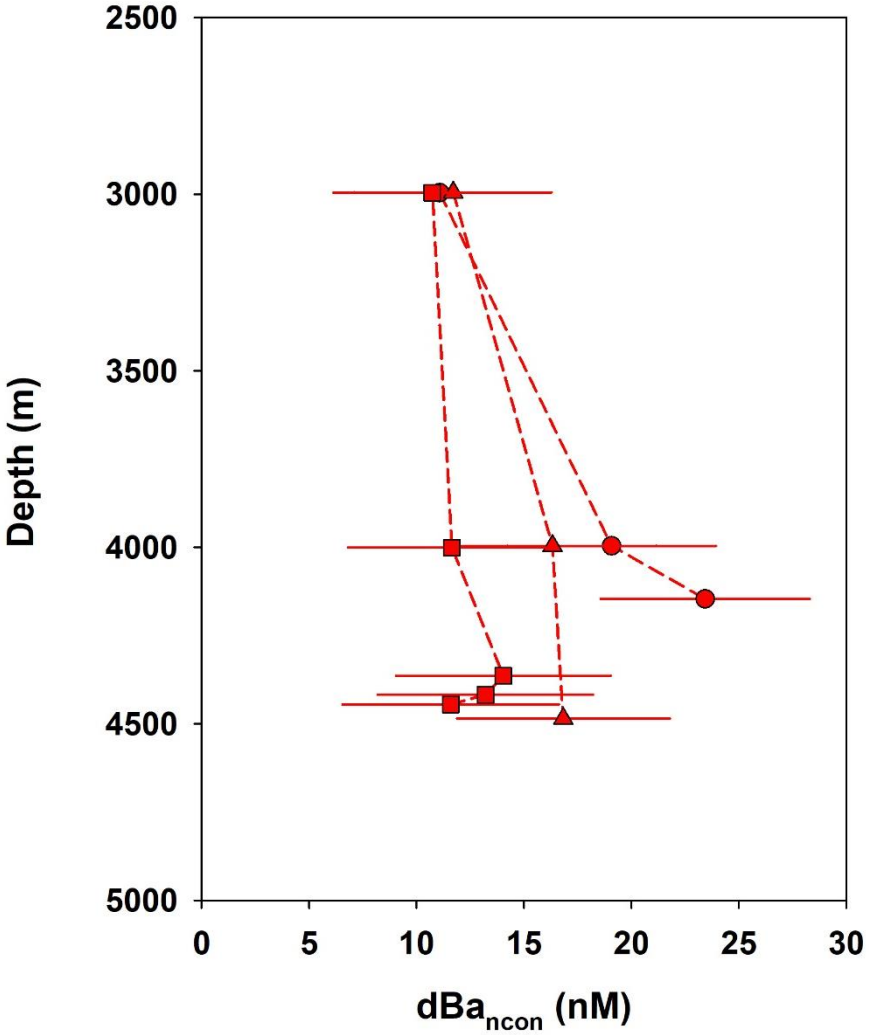

Figure S8. Nonconservative additions of dBa (dBa_{ncon}) below 2000m at off-shelf stations (Stn.21: circle; Stn.22: triangle; Stn.24: square).

Table S1. Summary of *in situ* dissolved barium concentration and isotopic composition in rivers (dBa_{river}, $\delta^{138}Ba_{river}$), estimated effective dissolved barium concentration and isotopic composition in rivers (dBa_{eff}, $\delta^{138}Ba_{eff}$), and the dissolved barium concentration maximum (dBa_{max}) in river plumes.

River estuary	**Amazon**	**Fly**	**Johor**	**Yangtze**	**Pearl**	**Congo**
Reference	(Bridgestock et al., 2021)			(Cao et al., 2021)		this study
dBa_{river} (nM)	124	143	352	232-405	152-199	123-136
$\delta^{138}Ba_{river}$ (‰)	0.15 ± 0.03	0.34 ± 0.19	0.19 ± 0.03	0.18-0.34	0.27-0.43	0.00-0.09
dBa_{eff} (nM)	268 ± 46	512 ± 74	1039 ± 318	450-565	235-265	204
$\delta^{138}Ba_{eff}$ (‰)	0.01 ± 0.06	0.11 ± 0.06	0.06 ± 0.12	0.1-0.2	0.1-0.2	-0.01-0.11
dBa_{max} (nM)	243	509	838	490	220-235	194

Dataset S1.

Dissolved barium and silicon isotopes at the Congo River-dominated Southeast Atlantic margin from METEOR cruise M121 (GEOTRACES cruise GA08): Dissolved barium (Ba) concentration and its stable isotopes, dissolved silicon (Si) concentration and its stable isotopes, and calculated Ba* values based on global, South Atlantic or regional (this study area) Si-Ba correlations. Ba* is defined as the deviation of dissolved Ba concentration from the Ba-Si linear relationship. Dataset link at PANGAEA: https://doi.pangaea.de/10.1594/PANGAEA.956054.